

Integral Equation Solution for Thermal Signatures of Buried Land Mines

İbrahim Kürşat Şendur and Brian A. Baertlein

The authors are with the ElectroScience Laboratory, Department of Electrical Engineering, The Ohio State University, Columbus, OH 43212-1191 USA. E-mail: baertlein.1@osu.edu .

Abstract

Predicting the thermal signature of a buried land mine requires modeling the complicated inhomogeneous environment and the structurally complex mine. It is useful, both in checking such models and in making rough calculations of expected signatures, to have an accurate, easily computed reference solution for a relatively simple geometry. In this paper a reference solution is presented for the time varying surface temperature distribution over a homogeneous cylindrical body (the mine model) buried in an infinite homogeneous half space (the soil model) with a planar interface. In this work the convection coefficient and air temperature are assumed to be time invariant and the radiation condition is linearized about its mean value. Using a periodic boundary condition in time at the planar interface, the temperature distribution in the lower-half space is expanded in a Fourier series. A volume integral equation for the Fourier series coefficients is obtained via Green's second identity, and the Green's function for the Fourier coefficients is derived. The solution procedure uses the method of weighted residuals (MWR), in which the integral equation is reduced to a matrix equation and then solved for the unknown temperature distribution. The integral equation solution is compared with a finite element method based model.

Keywords

Thermal infrared imagery, land mines, heat transfer, integral equations, thermal model, numerical simulation, Green's function, singularity extraction.

I. INTRODUCTION

Research in infrared (IR) detection of land mines has been ongoing for several decades, and those sensors (especially multi-spectral instruments) are considered promising. Although many experimental and empirical studies of IR mine detection have been performed, the physics that define IR signatures are poorly understood. These signatures are dependent on several factors, including solar insolation, cloud cover, vegetation, surface irregularities, and past meteorological conditions. There is a critical need to understand the effects of these environmental factors so that detection performance and sensor utilization can be improved.

Models for IR signatures of buried mines are not well developed, but there has been progress in modeling related problems. Thermal IR remote sensing of soil provides useful information for terrestrial studies such as characterizing geological materials, monitoring effusive volcanism, detecting fractures, and hazard assessment. Thermal IR data can also

provide valuable information about temporal and spatial variations of soil temperature, and soil temperature prediction has been widely studied in the literature using both analytical and numerical techniques. Those models are one-dimensional, but they describe heat transfer at the soil-air interface and various environmental processes that are critical components of three-dimensional thermal signature models. Watson [1] used a Fourier series formulation [2] for periodic heating of a surface to obtain an analytical solution for the temperature distribution in homogeneous soil heated by diurnal solar insolation. That work included the effects of skylight, atmospheric absorption, thermal radiation, and thermal conduction in soil. England et al. [3] included the effects of convective heat transfer between soil and air. Kahle [4] obtained a solution of the one-dimensional heat flow equation, including sensible and latent heat transfer. Watson [5] determined the surface temperature over a homogeneous layer by using the Laplace transform to obtain a relation between surface flux and surface temperature. England [6] used a one-dimensional model to study the radiometric characteristics of diurnally heated freezing and thawing soils. Liou and England [7] developed diurnal and annual models for freezing and thawing moist soils subject to annual insolation, radiant heating and cooling, and sensible and latent heat exchanges with the atmosphere. Liou and England [8] used a one-dimensional coupled heat and moisture transport model for bare, unfrozen, moist soils. They later extended the model to freezing soils [9].

Recently, thermal models of IR mine signatures have been described that offer a more complete understanding of the underlying physics. Sendur and Baertlein [10] used a one-dimensional analytical thermal model to predict the surface temperature distribution over a mine. The land mine is assumed to be buried under a layered earth subjected to diurnal solar heating. The analytical formulation is based on a Fourier analysis of the periodic phenomenon. Closed form expressions were derived for the temperature distribution on the soil surface and at depth. That simple analysis confirmed a number of results that are seen in experimental studies, including the presence of two thermal “cross-over” times, a lag between the solar illumination and the soil temperature, the attenuation of the signature strength with depth, and a marked difference in the signatures of thermally conducting and insulating buried objects.

In a companion paper, Sendur and Baertlein [11] developed a three-dimensional thermal model to predict surface temperatures over buried mines. That work is based on the finite element method (FEM), which is capable of modeling realistically shaped mines and inhomogeneous soil. Although a FEM approach to the problem appears very attractive, the accuracy and efficiency of such model bears investigation because of artificial boundaries required at the surface of the computational volume and discretization of the mine shape. An accurate and easily computed solution for a relatively simple geometry is desirable for checking the more detailed FEM models and for making rough calculations of more complex environments. In this paper we present an integral equation solution for a homogeneous cylindrical body (the mine model) buried in an infinite homogeneous half-space with a planar interface (the soil model). The model presented in this work uses a time invariant convection coefficient and air temperature. The solution of the volume integral equation is obtained using the method of weighted residuals (MWR), a technique also known to researchers in electromagnetics as the “Method of Moments (MoM)”. Although some derivations in this paper are inspired by work in electromagnetics, no knowledge of that subject is required here.

This work is organized as follows: Sect. II provides a description of the three-dimensional heat flow equation, including the convective and radiative boundary conditions at the soil-air interface. The Fourier series representation of the temperature distribution with appropriate boundary conditions is also presented in that section. In Sect. III integral representations for the temperature distribution in the soil and mine are obtained. The Green’s function for this problem is derived in Sect. IV and subsequently simplified and converted into a computationally efficient form. The numerical solution procedure for the Fourier series coefficients of the temperature distribution is formulated in Sect. V. Numerical results are presented in Sect. VI, and the integral-equation and FEM solutions are compared. Concluding remarks appear in Sect. VII.

II. FOURIER SERIES COEFFICIENTS OF TEMPERATURE DISTRIBUTION

The physical processes and the heat transfer mechanisms that produce IR signatures of buried land mines are discussed in a companion paper [11] and will not be repeated here. The key results are summarized below for the sake of completeness.

The temperature distribution in the soil and mine is described by the three-dimensional heat flow equation

$$C(\mathbf{r}) \frac{\partial T(\mathbf{r}, t)}{\partial t} = \nabla \cdot (\mathcal{K}(\mathbf{r}) \nabla T(\mathbf{r}, t)), \quad (1)$$

where $T(\mathbf{r}, t)$ [K] is the temperature distribution, \mathcal{K} [W m⁻¹ K⁻¹] is the thermal conductivity of the material, and C [J m⁻³ K⁻¹] is the volumetric heat capacity of the material. Previous research on thermal modeling of homogeneous soil [1, 3–9] has produced the linearized boundary condition at the soil-air interface

$$\frac{\partial T(\mathbf{r}, t)}{\partial z} \approx T(\mathbf{r}, t) \frac{1}{\mathcal{K}_s} (h(t) + 4\mathcal{E}\sigma T_{sky}^3(t)) - \frac{1}{\mathcal{K}_s} (\mathcal{F}_{sun}(t) + h(t)T_{air}(t) + 4\mathcal{E}\sigma T_{sky}^4(t)). \quad (2)$$

where \mathcal{F}_{sun} is the incident solar radiation reduced by cloud extinction, atmospheric absorption, soil albedo and the cosine of the zenith angle; T_{sky} and T_{air} are the sky and air temperatures, respectively; \mathcal{K}_s [W m⁻¹ K⁻¹] is the thermal conductivity of the soil; \mathcal{E} [unitless] is the mean emissivity of the surface; $\sigma = 5.67 \times 10^{-8}$ [W m⁻² K⁻⁴] is the Stefan-Boltzmann constant; and $h(t)$ is a convection coefficient.

In this paper we present an integral equation based solution to Eq. (1). The boundary condition at the soil-air interface given by Eq. (2) is time-varying. If the convection coefficient $h(t)$ is approximated by its mean value \bar{h} , then this boundary condition becomes a periodic function at the diurnal rate. This approximation suggests that the temperature distribution $T(\mathbf{r}, t)$ can be written as

$$T(\mathbf{r}, t) = \sum_{n=-\infty}^{\infty} T_n(\mathbf{r}) e^{i\omega n t} \quad (3)$$

where $\omega = 2\pi/(86400)$ [rad s⁻¹] is the radian frequency of a diurnal cycle and $T_n(\mathbf{r})$ is the n th Fourier coefficient of the temperature. Since $T(\mathbf{r}, t)$ is a real quantity, the coefficients satisfy $T_n(\mathbf{r}) = T_{-n}^*(\mathbf{r})$ where $*$ denotes the complex conjugate operator. Substituting Eq. (3) in Eq. (1) and assuming piecewise constant material properties, the Fourier coefficients of the three-dimensional heat-flux equation can be written as

$$\nabla^2 T_n(\mathbf{r}) - \frac{i\omega n}{\kappa_i(\mathbf{r})} T_n(\mathbf{r}) = 0, \quad i = s, m \quad (4)$$

Solar heating is the dominant heat source in this problem, and this fact permits additional approximations. Replacing $T_{air}(t)$ with its mean value \bar{T}_{air} , and simplifying T_{sky} in

a similar manner yields

$$\frac{\partial T(\mathbf{r}, t)}{\partial z} \approx T(\mathbf{r}, t) \frac{1}{\mathcal{K}_s} (\bar{h} + 4\mathcal{E}\sigma\bar{T}_{sky}^3) - \frac{1}{\mathcal{K}_s} (\mathcal{F}_{sun}(t) + \bar{h}\bar{T}_{air} + 4\mathcal{E}\sigma\bar{T}_{sky}^4) \quad (5)$$

By using a Fourier expansion of the solar insolation function

$$\mathcal{F}_{sun}(t) = \sum_{n=-\infty}^{\infty} \mathcal{F}_n e^{i\omega n t} \quad (6)$$

the boundary condition for the n th Fourier coefficient can be written as

$$\frac{\partial T_n(\mathbf{r})}{\partial z} = \alpha T_n(\mathbf{r}) + \beta_n \quad (7)$$

where

$$\alpha = (\bar{h} + 4\mathcal{E}\sigma\bar{T}_{sky}^3) / \mathcal{K}_s \quad (8)$$

$$\beta_n = -(\mathcal{F}_n + \bar{h}\bar{T}_{air} + 4\mathcal{E}\sigma\bar{T}_{sky}^4) / \mathcal{K}_s \quad (9)$$

III. INTEGRAL REPRESENTATION FOR THE TEMPERATURE DISTRIBUTION

In this section an integral representation for the Fourier coefficients of temperature in the lower half space will be obtained for a cylindrical mine with radius ρ_0 and thickness τ , buried at depth h under a smooth soil surface (see Fig. 1). Homogeneous soil with thermal diffusivity $\kappa_s(\mathbf{r}) = \kappa_s$ and thermal conductivity $\mathcal{K}_s(\mathbf{r}) = \mathcal{K}_s$ is assumed. The thermal properties of the mine need not be uniform in the following formulation, and the position (\mathbf{r}) dependence on the mine's thermal properties will be retained in this formulation.

A. Problem Formulation

For a mine that is a body of revolution, the problem has rotational symmetry. Therefore, Eq. (4) can be written as

$$\begin{aligned} \nabla_{\rho z}^2 T_n^s(\mathbf{r}) - k_n^2 T_n^s(\mathbf{r}) &= 0 ; \quad \mathbf{r} \in \text{soil} \\ \nabla_{\rho z}^2 T_n^m(\mathbf{r}) - \hat{k}_n^2(\mathbf{r}) T_n^m(\mathbf{r}) &= 0 ; \quad \mathbf{r} \in \text{mine} \end{aligned} \quad (10)$$

where

$$\nabla_{\rho z}^2 = \frac{1}{\rho} \frac{\partial}{\partial \rho} \left(\rho \frac{\partial}{\partial \rho} \right) + \frac{\partial^2}{\partial z^2} \quad (11)$$

$$k_n^2 = \frac{i\omega n}{\kappa_s} \quad (12)$$

$$\hat{k}_n^2(\mathbf{r}) = \frac{i\omega n}{\kappa_m(\mathbf{r})} \quad (13)$$

In Eq. (10) $T_n^m(\mathbf{r})$ and $T_n^s(\mathbf{r})$ represent the Fourier coefficients in the mine and soil regions, respectively.

We employ a standard method [12] of solving the differential operator equation defined in Eq. (4). Forming the inner product of that equation and the Green's function G yields

$$\langle \nabla_{\rho z}^2 T_n(\rho', z'), G(\rho, z; \rho', z') \rangle = \langle \nabla_{\rho z}^2 G(\rho, z; \rho', z'), T_n(\rho', z') \rangle + \mathcal{R}(\rho, z) \quad (14)$$

where $\langle \cdot, \cdot \rangle$ is the inner product, which comprises integration over the entire lower half space. The Green's function satisfies the equation

$$(\nabla_{\rho z}^2 - k_n^2)G(\rho, z; \rho', z') = -\frac{\delta(\rho - \rho')}{\rho} \delta(z - z') \quad (15)$$

with boundary conditions defined below. The conjunct \mathcal{R} is an integral over the problem boundaries [12, p. 198] and is also defined below. Using the above property of G and the differential equation satisfied by T_n we immediately obtain

$$T_n(\rho, z) = \int_{z_1}^{z_2} dz' \int_0^{\rho_0} d\rho' \rho' c(\rho', z') T_n(\rho', z') G(\rho, z; \rho', z') + \mathcal{R} \quad (16)$$

In this result $z_1 = h$, $z_2 = h + \tau$, we have exchanged primed and unprimed coordinates, and we have defined

$$c(\mathbf{r}) = \hat{k}_n^2(\mathbf{r}) - k_n^2 = i\omega n \frac{\kappa_s - \kappa_m(\mathbf{r})}{\kappa_s \kappa_m(\mathbf{r})} \quad (17)$$

Integration by parts is used to determine \mathcal{R} from its definition in Eq. (14). In doing so, we exploit the thermal boundary conditions, namely that temperature is continuous

$$T_n^m(\mathbf{r} = \mathbf{r}_{ms}) = T_n^s(\mathbf{r} = \mathbf{r}_{ms}) \quad (18)$$

and thermal flux is continuous

$$\mathcal{K}_m \nabla T_n^m(\mathbf{r}) \Big|_{\mathbf{r}=\mathbf{r}_{ms}} = \mathcal{K}_s \nabla T_n^s(\mathbf{r}) \Big|_{\mathbf{r}=\mathbf{r}_{ms}} \quad (19)$$

where \mathbf{r}_{ms} denotes any point on the mine-soil boundary. The following result is obtained

$$\begin{aligned} \mathcal{R}(\rho, z) &= - \int_0^\infty d\rho' \rho' \mathcal{Z}^s(\rho, z; \rho', 0) + \rho_0 \int_{z_1}^{z_2} dz' \mathcal{F}^m(\rho, z; \rho_0, z') \left(1 - \frac{\mathcal{K}_m(\rho_0, z')}{\mathcal{K}_s}\right) \\ &+ \int_0^{\rho_0} d\rho' \rho' \left(\mathcal{S}^m(\rho, z; \rho', z_2) \left(1 - \frac{\mathcal{K}_m(\rho', z_2)}{\mathcal{K}_s}\right) \right. \\ &\quad \left. - \mathcal{S}^m(\rho, z; \rho', z_1) \left(1 - \frac{\mathcal{K}_m(\rho', z_1)}{\mathcal{K}_s}\right) \right) \end{aligned} \quad (20)$$

in which

$$\mathcal{Z}^i(\rho, z; \rho', z') = \mathcal{S}^i(\rho, z; \rho', z') - T_n^i(\rho', z') \frac{\partial G(\rho, z; \rho', z'')}{\partial z''} \Big|_{z''=z'} \quad (21)$$

$$\mathcal{F}^i(\rho, z; \rho', z') = G(\rho, z; \rho', z') \frac{\partial T_n^i(\rho'', z')}{\partial \rho''} \Big|_{\rho''=\rho'} \quad (22)$$

$$\mathcal{S}^i(\rho, z; \rho', z') = G(\rho, z; \rho', z') \frac{\partial T_n^i(\rho', z'')}{\partial z''} \Big|_{z''=z'} \quad (23)$$

In Eqs. (21)-(23) the subscript i can be s or m , which refer to the soil and mine, respectively. By selecting the following boundary condition for the Green's function at the soil-air interface

$$\frac{\partial G(\rho, z; \rho', z')}{\partial z} = \alpha G(\rho, z; \rho', z') \quad (24)$$

the integral representation for the temperature distribution $T_n(\rho, z)$ in the lower half space can be obtained as

$$\begin{aligned} T_n(\rho, z) &= - \int_{z_1}^{z_2} dz' \int_0^{\rho_0} d\rho' \rho' c(\rho', z') T_n^m(\rho', z') G(\rho, z; \rho', z') \\ &- \beta_n \int_0^\infty d\rho' \rho' G(\rho, z; \rho', z' = 0) + \rho_0 \int_{z_1}^{z_2} dz' \mathcal{F}^m(\rho, z; \rho_0, z') \left(1 - \frac{\mathcal{K}_m(\rho_0, z')}{\mathcal{K}_s}\right) \\ &+ \int_0^{\rho_0} d\rho' \rho' \left(\mathcal{S}^m(\rho, z; \rho', z_2) \left(1 - \frac{\mathcal{K}_m(\rho', z_2)}{\mathcal{K}_s}\right) \right. \\ &\quad \left. - \mathcal{S}^m(\rho, z; \rho', z_1) \left(1 - \frac{\mathcal{K}_m(\rho', z_1)}{\mathcal{K}_s}\right) \right) \end{aligned} \quad (25)$$

Equation (25) is an integral relation from which one can determine the temperature distribution anywhere in the lower half space by integrating the temperature distribution over the mine. If (ρ, z) is a point within the mine, this relation is a Fredholm's integral equation of the second kind for the unknown mine temperature distribution. In the absence of the

mine, i.e., for a homogeneous half space, the first, third, and last terms in Eq. (25) vanish and the temperature distribution can be found directly from

$$T_n(\rho, z) = -\beta_n \int_0^\infty d\rho' \rho' G(\rho, z; \rho', z' = 0) \quad (26)$$

The Green's function for Eq. (25) is derived in Sect. IV. The numerical solution procedure for Eq. (25) is presented in Sect. V.

B. Alternative Interpretation

An alternative view of the problem offers a physical interpretation of the expressions derived in Sect. III-A, and it permits analysis of mines containing media that are not piecewise constant. The key mathematical tool in this work is the volume equivalence theorem for the heat transfer equation. The volume equivalence theorem is widely used in electromagnetics [13–15] to determine the scattered electromagnetic fields in the presence of a material body in a homogeneous environment.

The original problem comprises a buried mine with thermal properties $\kappa_m(\mathbf{r})$ and $\mathcal{K}_m(\mathbf{r})$ in homogeneous soil with thermal properties $\kappa_s(\mathbf{r}) = \kappa_s$ and $\mathcal{K}_s(\mathbf{r}) = \mathcal{K}_s$. A new equivalent problem can be defined in which the mine is replaced by homogeneous soil and an equivalent heat source $\mathcal{Q}(\mathbf{r})$ as shown in Fig. 2. The temperature anomaly due to the inhomogeneity can be viewed as being generated by a so-called “induced” source $\mathcal{Q}(\mathbf{r})$, which is proportional to the temperature distribution in the inhomogeneous volume. The derivation is well known in electromagnetics, but somewhat involved. Using Eq. (3) in Eq. (1) and the properties of the divergence operator, we obtain

$$\mathcal{K}(\mathbf{r}) \nabla^2 T_n(\mathbf{r}) + \nabla \mathcal{K}(\mathbf{r}) \cdot \nabla T_n(\mathbf{r}) - i\omega n C(\mathbf{r}) T_n(\mathbf{r}) = 0 \quad (27)$$

Dividing both sides of Eq. (27) by $\mathcal{K}(\mathbf{r})$ we get

$$\nabla^2 T_n(\mathbf{r}) + \frac{\nabla \mathcal{K}(\mathbf{r})}{\mathcal{K}(\mathbf{r})} \cdot \nabla T_n(\mathbf{r}) - k^2(\mathbf{r}) T_n(\mathbf{r}) = 0 \quad (28)$$

where

$$k^2(\mathbf{r}) = i\omega n \frac{C(\mathbf{r})}{\mathcal{K}(\mathbf{r})} = k_n^2 + (\hat{k}_n^2(\mathbf{r}) - k_n^2) U_{mine}(\mathbf{r}) \quad (29)$$

where k_n^2 and $\hat{k}_n^2(\mathbf{r})$ are defined in Sect. III-A and

$$U_{mine}(\mathbf{r}) = \begin{cases} 1 & ; \mathbf{r} \in \text{mine} \\ 0 & ; \mathbf{r} \in \text{soil} \end{cases} \quad (30)$$

Substituting Eq. (30) into Eq. (28) and rearranging the terms yields

$$\nabla^2 T_n(\mathbf{r}) - k_n^2 T_n(\mathbf{r}) = \mathcal{Q}(\mathbf{r}) \quad (31)$$

where $\mathcal{Q}(r)$ is the fictitious heat source. This is given by two terms

$$\mathcal{Q}(\mathbf{r}) = \mathcal{Q}_v(\mathbf{r}) + \mathcal{Q}_s(\mathbf{r}) \quad (32)$$

where

$$\mathcal{Q}_v(\mathbf{r}) = c(\mathbf{r})T_n(\mathbf{r})U_{mine}(\mathbf{r}) \quad (33)$$

$$\mathcal{Q}_s(\mathbf{r}) = -\frac{\nabla \mathcal{K}(\mathbf{r})}{\mathcal{K}(\mathbf{r})} \cdot \nabla T_n(\mathbf{r}) \quad (34)$$

The quantity $c(\mathbf{r})$ in Eq. (33) has been defined in Sect. III-A. Also note that

$$\begin{aligned} \frac{\nabla \mathcal{K}(\mathbf{r})}{\mathcal{K}(\mathbf{r})} &= \left(1 - \frac{\mathcal{K}_m(\rho, z_1)}{\mathcal{K}_s}\right) \delta(z - z_1) \left(u(\rho) - u(\rho - \rho_0)\right) \hat{z} \\ &- \left(1 - \frac{\mathcal{K}_m(\rho, z_2)}{\mathcal{K}_s}\right) \delta(z - z_2) \left(u(\rho) - u(\rho - \rho_0)\right) \hat{z} \\ &- \left(1 - \frac{\mathcal{K}_m(\rho_0, z)}{\mathcal{K}_s}\right) \delta(\rho - \rho_0) \left(u(z - z_1) - u(z - z_2)\right) \hat{\rho} \end{aligned} \quad (35)$$

where u is the unit step function. Eq. (31) can be manipulated to yield a volume integral equation, which can be solved for the unknown, induced heat source. Using this induced heat source, the temperature distribution in the lower half space can be found by integration. This volume formulation can be conveniently used to treat any inhomogeneous material, not just the piecewise constant media discussed here.

Applying Green's second identity to the functions $T_n(\rho, z)$ and $G(\rho, z; \rho', z')$ with a source distribution $\mathcal{Q}(\rho, z)$ in the mine gives

$$\begin{aligned} T_n(\rho, z) &= -\int_{z_1}^{z_2} dz' \int_0^{\rho_0} d\rho' \rho \mathcal{Q}(\rho', z') G(\rho, z; \rho', z') \\ &+ \int_{\Gamma} \left[T_n(\rho, z) \nabla G(\rho, z; \rho', z') - G(\rho, z; \rho', z') \nabla T_n(\rho, z) \right] \cdot \hat{n} dS \end{aligned} \quad (36)$$

where Γ denotes the boundaries (at the soil-air interface and at the mine) and \hat{n} is the unit normal on those boundaries. Using the definitions of the boundaries, Eq. (36) can be written as

$$T_n(\rho, z) = - \int_{z_1}^{z_2} dz' \int_0^{\rho_0} d\rho' \rho \mathcal{Q}(\rho', z') G(\rho, z; \rho', z') - \int_0^\infty d\rho' \rho' \mathcal{Z}^s(\rho, z; \rho', 0) \quad (37)$$

Equation (37) can be transformed into Eq. (25) by selecting the boundary condition for G as given by Eq. (24).

IV. GREEN'S FUNCTION

The Green's function G is the solution of the heat transfer equation for an internal point source of heat. When G is known, a solution for an arbitrary source can be obtained via Eq. (25). In this section a Green's function will be derived, which satisfies Eq. (15) with the boundary condition on the soil-air interface given by Eq. (24). In addition to this boundary condition, the Green's function must have a finite value for $G(\rho = 0, z; \rho', z')$ and must vanish as $\rho \rightarrow \infty$ and $z \rightarrow \infty$. In Sect. IV-A the derivation is presented. In Sect. IV-B the Green's function is simplified and transformed into a more appropriate form for numerical evaluation.

A. Derivation of the Green's Function

The Green's function is easily derived in the spectral domain. Taking the Hankel transform [12]

$$\hat{f}(k_\rho) = \int_0^\infty x J_0(k_\rho x) f(x) dx \quad (38)$$

of both sides of the Eq. (15) we obtain

$$\left(\frac{\partial^2}{\partial z^2} - (k_\rho^2 + k_n^2) \right) \hat{G}(k_\rho, z; \rho', z') = -J_0(k_\rho \rho') \delta(z - z') \quad (39)$$

where $\hat{G}(k_\rho, z; \rho', z')$ is the Hankel transform of the Green's function $G(\rho, z; \rho', z')$. In obtaining Eq. (39) the differential equation for the zeroth order Bessel function was used. The solution of the ordinary differential equation given by Eq. (39) with the boundary conditions at the interface can be obtained through well known methods. We can show

$$\frac{\hat{G}(k_\rho, z; \rho', z')}{J_0(k_\rho \rho')} = \frac{1}{2\sqrt{k_n^2 + k_\rho^2}} \exp\left(-\sqrt{k_n^2 + k_\rho^2} z_{>}\right) \left[\exp\left(\sqrt{k_n^2 + k_\rho^2} z_{<}\right) \right]$$

$$+r_0(k_n, k_\rho, \alpha) \exp\left(-\sqrt{k_n^2 + k_\rho^2} z_{<}\right) \Big] \quad (40)$$

where

$$r_0(k_n, k_\rho, \alpha) = \frac{\sqrt{k_n^2 + k_\rho^2} - \alpha}{\sqrt{k_n^2 + k_\rho^2} + \alpha} \quad (41)$$

The inverse Hankel transform, given by

$$f(x) = \int_0^\infty k_\rho J_0(k_\rho x) \hat{f}(k_\rho) dk_\rho \quad (42)$$

yields the desired result

$$\begin{aligned} G(\rho, z; \rho', z') &= \int_0^\infty dk_\rho J_0(k_\rho \rho') J_0(k_\rho \rho) \frac{k_\rho}{2\sqrt{k_n^2 + k_\rho^2}} \exp\left(-\sqrt{k_n^2 + k_\rho^2} z_{>}\right) \\ &\times \left[\exp\left(\sqrt{k_n^2 + k_\rho^2} z_{<}\right) + r_0(k_n, k_\rho, \alpha) \exp\left(-\sqrt{k_n^2 + k_\rho^2} z_{<}\right) \right] \end{aligned} \quad (43)$$

B. Simplification of the Green's Function

Numerical evaluation of the Green's function given by Eq. (43) is computationally challenging. The integral in Eq. (43) is similar to the Sommerfeld integrals [16], which have been studied extensively in the physics and electromagnetics literature. The major difficulties in the computation of these integrals can be summarized as follows:

- For large argument x , the function $J_0(x)$ oscillates rapidly, leading to slow convergence.
- For $|z - z'| \ll 1$ or $(z + z') \ll 1$ the exponential terms in the integrals decay slowly, again producing slow convergence.

Straightforward manipulations ameliorate some of these problems. The quantity $r_0(k_n, k_\rho, \alpha)$ can be expressed as

$$r_0(k_n, k_\rho, \alpha) = 1 - \frac{2\alpha}{\sqrt{k_n^2 + k_\rho^2} + \alpha} \quad (44)$$

and, hence, the Green's function can be expressed as

$$G(\rho, z; \rho', z') = G_1(\rho, z; \rho', z') + G_2(\rho, z; \rho', z') + G_3(\rho, z; \rho', z') \quad (45)$$

where

$$G_1(\rho, z; \rho', z') = \int_0^\infty dk_\rho J_0(k_\rho \rho') J_0(k_\rho \rho) \frac{k_\rho}{2\sqrt{k_n^2 + k_\rho^2}} \exp\left(-\sqrt{k_n^2 + k_\rho^2} (z_{>} - z_{<})\right) \quad (46)$$

$$G_2(\rho, z; \rho', z') = \int_0^\infty dk_\rho J_0(k_\rho \rho') J_0(k_\rho \rho) \frac{k_\rho}{2\sqrt{k_n^2 + k_\rho^2}} \exp\left(-\sqrt{k_n^2 + k_\rho^2}(z + z')\right) \quad (47)$$

$$G_3(\rho, z; \rho', z') = -\alpha \int_0^\infty dk_\rho J_0(k_\rho \rho') J_0(k_\rho \rho) \frac{k_\rho}{\sqrt{k_n^2 + k_\rho^2}(\sqrt{k_n^2 + k_\rho^2} + \alpha)} \exp\left(-\sqrt{k_n^2 + k_\rho^2}(z + z')\right) \quad (48)$$

Employing the multiplication identity for the zeroth order Bessel functions used by Johnson [17]

$$J_0(k_\rho \rho') J_0(k_\rho \rho) = \frac{1}{2\pi} \int_0^{2\pi} J_0(k_\rho \rho_t) d\phi \quad (49)$$

where

$$\rho_t = \sqrt{\rho^2 + \rho'^2 - 2\rho\rho' \cos \phi} \quad (50)$$

and changing the order of integration we can rewrite Eqs. (46) and (47) as

$$G_1(\rho, z; \rho', z') = \frac{1}{4\pi} \int_0^{2\pi} d\phi' \int_0^\infty dk_\rho J_0(k_\rho \rho_t) \frac{k_\rho}{\sqrt{k_n^2 + k_\rho^2}} \exp\left(-\sqrt{k_n^2 + k_\rho^2}(z_{>} - z_{<})\right) \quad (51)$$

$$G_2(\rho, z; \rho', z') = \frac{1}{4\pi} \int_0^{2\pi} d\phi' \int_0^\infty dk_\rho J_0(k_\rho \rho_t) \frac{k_\rho}{\sqrt{k_n^2 + k_\rho^2}} \exp\left(-\sqrt{k_n^2 + k_\rho^2}(z + z')\right) \quad (52)$$

Using the following identity [12]

$$\frac{\exp(-k\sqrt{r^2 + z^2})}{\sqrt{r^2 + z^2}} = \int_0^\infty \gamma J_0(\gamma r) \frac{\exp(-|z|\sqrt{k^2 + \gamma^2})}{\sqrt{k^2 + \gamma^2}} d\gamma \quad (53)$$

permits Eqs. (51) and (52) to be simplified to

$$G_m(\rho, z; \rho', z') = \int_0^{2\pi} d\phi' \frac{\exp(ik_n R_m)}{4\pi R_m}; \quad m = 1, 2 \quad (54)$$

where

$$R_1 = \sqrt{\rho'^2 + \rho^2 - 2\rho'\rho \cos \phi' + (z - z')^2} \quad (55)$$

$$R_2 = \sqrt{\rho'^2 + \rho^2 - 2\rho'\rho \cos \phi' + (z + z')^2} \quad (56)$$

Similarly, substituting Eq. (49) into Eqs. (57) and changing the order of integration we obtain

$$G_3(\rho, z; \rho', z') = -\frac{\alpha}{2\pi} \int_0^{2\pi} d\phi I_{G_3} \quad (57)$$

where

$$I_{G_3} = \int_0^\infty dk_\rho J_0(k_\rho \rho_t) \frac{k_\rho}{\sqrt{k_n^2 + k_\rho^2} (\sqrt{k_n^2 + k_\rho^2} + \alpha)} \exp\left(-\sqrt{k_n^2 + k_\rho^2}(z + z')\right) \quad (58)$$

We can express this in another form as suggested by Kuo and Mei [18]. Multiplying both sides of Eq. (58) by $\exp(-\alpha(z + z'))$ and differentiating with respect to $z + z'$ yields

$$\frac{\partial(I_{G_3} \exp(-\alpha(z + z')))}{\partial(z + z')} = -\exp(-\alpha(z + z')) \int_0^\infty dk_\rho J_0(k_\rho \rho_t) \frac{k_\rho}{\sqrt{k_n^2 + k_\rho^2}} \exp\left(-\sqrt{k_n^2 + k_\rho^2}(z + z')\right) \quad (59)$$

The integral in Eq. (59) can be evaluated using Eq. (53). After integrating both sides with respect to z over appropriate limits, I_{G_3} can be written as

$$I_{G_3} = \exp(-\alpha(z + z')) \int_{z+z'}^\infty \frac{\exp(ik_n R_3)}{R_3} \exp(-\alpha\zeta) d\zeta \quad (60)$$

where

$$R_3 = \sqrt{\rho'^2 + \rho^2 - 2\rho'\rho \cos \phi' + \zeta^2} \quad (61)$$

Using Eqs. (54), (57), and (60) in conjunction with Eq. (45) we obtain the final form of the Green's function as

$$G(\rho, z; \rho', z') = \int_0^{2\pi} d\phi' \frac{\exp(ik_n R_1)}{4\pi R_1} + \int_0^{2\pi} d\phi' \frac{\exp(ik_n R_2)}{4\pi R_2} - \frac{\alpha}{2\pi} \int_0^{2\pi} d\phi \exp(-\alpha(z + z')) \int_{z+z'}^\infty d\zeta \frac{\exp(ik_n R_3)}{R_3} \exp(-\alpha\zeta) \quad (62)$$

The last integral in Eq. (62) has infinite integration limits, but the integrand is a rapidly decaying function for typical values of α , and it is well approximated by an integral over a finite domain. When the source and observation points approach one another, we have $R_1 \rightarrow 0$, and the Green's function has a well-known integrable singularity. The treatment of this case is discussed in Sect. V-B and Appendix A.

V. NUMERICAL SOLUTION PROCEDURE

In this section we describe a numerical solution procedure for the integral equation in Eq. (25) to obtain the Fourier coefficients $T_n^m(\mathbf{r})$. Our approach is to solve for the temperature T_n^m within the mine, which can be used to evaluate Eq. (25) for the Fourier

coefficients at the surface. The time history of the temperature is then found by evaluating the Fourier series.

We employ the MWR in this work. As noted above, the electromagnetics community has developed an extensive body of knowledge on MWR solutions of integral equations in the temporal frequency domain under the guise of the so-called “method of moments” (MoM). The MoM discretizes the integral equation into a matrix equation, the solution of which is obtained using standard methods. Following the pioneering works of Richmond [19] and Harrington [20], an extensive literature has developed on this procedure, and good summary references are also available [21–23].

A. Matrix formulation

The solution of the integral equation using the MWR begins with a representation of the unknown temperature distribution over the buried mine using specified expansion functions and unknown coefficients. The problem at hand imposes constraints on these functions. The integral representation of the temperature distribution given in Eq. (25) requires both the temperature and its derivatives with respect to ρ and z . We employ expansion functions $\Lambda(\rho, z)$ that are linear in ρ and z , viz:

$$T_n^m(\rho, z) = \sum_{m=1}^M \sum_{n=1}^N A_{m,n} \Lambda_{nm}(\rho, z) \quad (63)$$

where M and N are the number of divisions in the z and ρ directions, respectively. This representation yields a continuous, piecewise-linear representation of T_n^m and a piecewise constant form for its derivatives.

A sample discretization of the buried mine with $N = 4$ subdivisions in the $\hat{\rho}$ -direction and $M = 3$ subdivisions in the \hat{z} -direction is illustrated in Fig. 3. The thermal properties over each subsectional basis function are assumed constant and taken into account in the constant $c_{m,n}$, which can be defined as

$$c_{m,n} = c((\rho_n + \rho_{n-1})/2, (z_m + z_{m-1})/2) \quad (64)$$

where c was previously defined in Eq. (17) and the indexed values ρ_n and z_m are the subsection boundaries. By substituting the approximate temperature distribution of Eq. (63)

into the integral equation Eq. (25), we obtain

$$\begin{aligned}
\beta_n \int_0^\infty d\rho' \rho' G(\rho, z; \rho', z' = 0) &= - \sum_{m=1}^M \sum_{n=1}^N A_{mn} [\Lambda_{mn}(\rho, z) \\
&\quad + c_{mn} \int \int dz' d\rho' \rho' G(\rho, z; \rho', z') \Lambda_{mn}(\rho', z')] \\
+ \rho_0 \sum_{m=1}^M A_{mN} \int dz' G(\rho, z; \rho' = \rho_0, z') \cdot \\
&\quad \frac{d}{d\rho'} \Lambda_{nm}(\rho', z') \left(1 - \frac{\mathcal{K}_m(\rho_0, z')}{\mathcal{K}_s}\right) \\
+ \sum_{n=1}^N A_{Mn} \int d\rho' \rho' G(\rho, z; \rho', z' = z_2) \cdot \\
&\quad \frac{d}{dz'} \Lambda_{nm}(\rho', z') \left(1 - \frac{\mathcal{K}_m(\rho', z_2)}{\mathcal{K}_s}\right) \\
- \sum_{n=1}^N A_{1n} \int d\rho' \rho' G(\rho, z; \rho', z' = z_1) \cdot \\
&\quad \frac{d}{dz'} \Lambda_{nm}(\rho', z') \left(1 - \frac{\mathcal{K}_m(\rho', z_1)}{\mathcal{K}_s}\right) \tag{65}
\end{aligned}$$

To complete the formulation, we express the left-hand side of Eq. 65 using the summation in Eq. (63), multiply both sides of Eq. (65) by testing functions $w_{n'm'}(\rho, z)$ and integrate over the mine. Various testing functions have been used in the literature. Galerkin methods are known to be optimum in the least-square sense, but for integral equations they are also computationally expensive in terms of matrix-fill time. To reduce the computational cost, we have employed a point-matching technique. The result can be expressed as a linear system of equations

$$\bar{\mathbf{Z}} \mathbf{A} = \mathbf{V} \tag{66}$$

for the constants A_{mn} , which we represent by the matrix \mathbf{A} . The kernel of the integral equation appears in $\bar{\mathbf{Z}}$ which we refer to as the ‘‘impedance’’ matrix. Solving Eq. (66) using an appropriate technique yields the unknown coefficient vector \mathbf{A} , which can be used to compute the temperature distribution over the buried mine via Eq. (63). If desired, the temperature distribution everywhere in the lower half-space can be computed using Eq. (25).

B. Impedance matrix, source vector, and singularity extraction

In this section evaluation of the matrix $\bar{\mathbf{Z}}$ is discussed. Rows of this matrix have indices derived from the (ρ, z) expansion functions indexed by m and n , with a similar relation for the columns involving ρ' and z' . To make the notation more concise, we use the index p to refer to a particular point (ρ, z) , which we denote (ρ_{n_p}, z_{m_p}) with a similar convention for ρ' and z' using q . In general, Z_{pq} involves integrals of the form

$$\int_{z_{m_q-1}}^{z_{m_q}} dz' \int_{\rho_{n_q-1}}^{\rho_{n_q}} d\rho' G(\rho_{n_p}, z_{m_p}; \rho', z') f(\rho', z') \quad (67)$$

where $f(\rho, z)$ is a continuous (at most linear) function of the arguments. Consider first the off-diagonal matrix elements Z_{pq} with $p \neq q$. For this case, the testing point (ρ_{n_p}, z_{m_p}) is not in the integration domain and the Green's function is a smooth function. In this case Z_{pq} can be directly evaluated by numerical methods.

For the diagonal matrix elements Z_{pp} , however, the testing point (ρ_{n_p}, z_{m_p}) lies in the integration domain. This results in $R_1 \rightarrow 0$ which causes a singularity as R_1^{-1} . Consequently, an integrand regularization technique (e.g., singularity extraction) is necessary in numerical evaluation of the integrals. Singularity extraction techniques are widely used in MoM solutions in electromagnetics for both surface and volume formulations [24–27]. Techniques for bodies of revolution have also been studied [28, 29], which are now described.

In brief, calculation of the diagonal elements requires that the singular parts of the integrand are evaluated separately by analytical methods. A careful examination suggests that the singular part of the Green's function $G(\rho, z; \rho', z')$ is due to function $G_1(\rho, z; \rho', z')$, which leads us to write

$$G_1(\rho, z; \rho', z') = G_1^R(\rho, z; \rho', z') + \int_0^{2\pi} d\phi' \frac{1}{4\pi R_1} f(\rho, z) \quad (68)$$

where $f(\rho, z)$ is a smooth function and

$$G_1^R(\rho, z; \rho', z') = \int_0^{2\pi} d\phi' \frac{\exp(ik_n R_1) - 1}{4\pi R_1} \quad (69)$$

The function $G_1^R(\rho, z; \rho', z')$ can be integrated numerically. For small elements a Taylor series expansion of the integrand yields

$$\lim_{R_1 \rightarrow 0} G_1^R(\rho, z; \rho', z') = \frac{k_n}{2} \quad (70)$$

The remaining singular integral in Eq. (68) has one of the following forms

$$\begin{bmatrix} I_c(\rho_l, \rho_u; \phi_l, \phi_u; z_l, z_u) \\ I_\rho(\rho_l, \rho_u; \phi_l, \phi_u; z_l, z_u) \\ I_z(\rho_l, \rho_u; \phi_l, \phi_u; z_l, z_u) \end{bmatrix} = \int_{\rho_l}^{\rho_u} d\rho' \rho' \int_{z_l}^{z_u} dz' \int_{\phi_l}^{\phi_u} d\phi' \cdot \frac{1}{\sqrt{\rho'^2 + \rho^2 - 2\rho'\rho \cos \phi' + (z - z')^2}} \begin{bmatrix} 1 \\ \rho' \\ z' \end{bmatrix} \quad (71)$$

Evaluation of these functions is discussed in Appendix I.

Singularity extraction is not necessary in evaluating the source vector elements V_p , since $G(\rho, z; \rho', z')$ is evaluated at the testing point $z_{mp} > 0$ while $z' = 0$.

C. Surface Temperature Distribution

The numerical procedure described in Sect. V-A yields the Fourier coefficients of the temperature distribution within the mine. The temperature distribution over the soil surface $z = 0$ is found by using Eqs. (3) and (65). The procedure offers some challenges. When $z = z' = 0$, the exponential factors in Eq. (62) are eliminated, leading to slow convergence. It is shown in Appendix II that an approximate but accurate and efficient form for the Green's function is

$$\begin{aligned} G(\rho, z = 0; \rho', z' = 0) &= \frac{1}{2\pi} \int_0^{2\pi} d\phi' \frac{\exp(ik_n \rho t)}{\rho_t} - \alpha K_0(-ik_n \rho_{>}) I_0(-ik_n \rho_{<}) \\ &- \frac{\alpha^2}{2\pi} \int_0^{2\pi} d\phi' \frac{\exp(ik_n \rho t)}{ik_n} - \frac{\alpha^3}{4\pi} \int_0^{2\pi} d\phi' \frac{\rho_t K_{-1}(-ik_n \rho t)}{ik_n} \end{aligned} \quad (72)$$

The Green's function representation given by Eq. (72) is used to evaluate the third term in Eq. (65) when the observation point is on the soil surface.

VI. RESULTS

In this section numerical simulation results are presented to compare the three-dimensional modeling capabilities of the integral equation solution with those of the FEM based solution. Additional results comparing these methods are given in a companion paper [11], where we considered several cases including a circular TNT-filled anti-tank mine simulant of diameter 20 cm and height 7.5 cm buried 4.5 cm under a perfectly smooth soil surface.

In this work, consider the simple case of circular cylinder of diameter 20 cm, height 7.5 cm, and depth 4.5 cm filled with a good thermal insulator (styrofoam).

An important parameter of this problem is the required number of harmonics in the Fourier expansion given by Eq. (3). The forcing function of this integral equation is the solar insolation function $\mathcal{F}_{sun}(t)$, the Fourier series of which is dominated by its first term. Therefore, we expect the temperature coefficients T_n to be rapidly convergent. Our numerical simulations support this expectation. An example Fourier harmonic distribution is given in Table I. Based on our numerical experiments, we kept the first five Fourier harmonics in the expansion given by Eq. (3).

TABLE I
FOURIER HARMONICS OF THE TEMPERATURE DISTRIBUTION AT A POINT OVER THE MINE

Harmonic #	T_n	$ T_n / T_1 $
1	$2.5351 + j3.8669$	1
2	$0.3582 + j1.3392$	0.2998
3	$0.0042 + j0.0945$	0.0205
4	$0.0140 - j0.1289$	0.0280
5	$0.0059 - j0.0248$	0.0055
6	$-0.0058 + j0.0120$	0.0029
7	$-0.0043 + j0.0094$	0.0022

Figure 4 shows the surface temperature over the center of the mine as a function of time. The FEM results are compared with those obtained via the integral equation method. The results show good agreement between the codes. In the second set of results, we investigated spatial variations in the surface temperature, by plotting the temperature along a cut through the center of the mine. We present the temperature at times that correspond to maximum signature contrast. Figure 5 illustrates the spatial distribution results. The FEM and integral equation models show good agreement. The integral equation solution took about 2 hours on a 300 MHz Pentium II machine. Most of this time is used to fill and factor the $\bar{\mathbf{Z}}$ matrix. The FEM solution took about 1 hour 40

minutes in the same machine. No significant attempts have been made to optimize either code.

VII. CONCLUSIONS

An integral-equation has been formulated for the temperature over a buried land mine. Using the approximations of a time invariant convection coefficient and air temperature, and linearizing the radiation boundary condition about its average value, the case of periodic (diurnal) solar heating leads to a Fourier decomposition of the time variation. The integral equation for each Fourier component of the temperature distribution was solved using the method of weighted residuals. The resulting model provides a reference solution for a relatively simple geometry, which can be used to check more sophisticated FEM-based models.

APPENDIX

I. ANALYTICAL TREATMENT OF THE SINGULAR INTEGRAL

In this appendix we evaluate the functions I_c , I_ρ , and I_z which were introduced in Eq. (71). Singularity extraction is required in the evaluation of these functions if the testing point lies in the integration domain. The boundaries of this integral and the location of the singularity are illustrated in Fig. 6.

Consider a small volume around the singularity. Such a volume can be defined by the cylindrical coordinates $\rho \in (\rho - \epsilon_\rho, \rho + \epsilon_\rho)$, $\phi \in (\phi - \epsilon_\phi, \phi + \epsilon_\phi)$, and $z \in (z - \epsilon_z, z + \epsilon_z)$. Figure 7 demonstrates the top and side views of this volume. The functions can be written as

$$\begin{aligned} \begin{bmatrix} I_c(\rho_1, \rho_2; 0, 2\pi; z_1, z_2) \\ I_\rho(\rho_1, \rho_2; 0, 2\pi; z_1, z_2) \\ I_z(\rho_1, \rho_2; 0, 2\pi; z_1, z_2) \end{bmatrix} &= \begin{bmatrix} I_c(\rho_1, \rho_2; 0, 2\pi; z_1, z - \epsilon_z) \\ I_\rho(\rho_1, \rho_2; 0, 2\pi; z_1, z - \epsilon_z) \\ I_z(\rho_1, \rho_2; 0, 2\pi; z_1, z - \epsilon_z) \end{bmatrix} \\ &+ \begin{bmatrix} I_c(\rho_1, \rho_2; 0, 2\pi; z + \epsilon_z, z_2) \\ I_\rho(\rho_1, \rho_2; 0, 2\pi; z + \epsilon_z, z_2) \\ I_z(\rho_1, \rho_2; 0, 2\pi; z + \epsilon_z, z_2) \end{bmatrix} \end{aligned}$$

$$\begin{aligned}
& + \begin{bmatrix} I_c(\rho_1, \rho - \epsilon_\rho; 0, 2\pi; z - \epsilon_z, z + \epsilon_z) \\ I_\rho(\rho_1, \rho - \epsilon_\rho; 0, 2\pi; z - \epsilon_z, z + \epsilon_z) \\ I_z(\rho_1, \rho - \epsilon_\rho; 0, 2\pi; z - \epsilon_z, z + \epsilon_z) \end{bmatrix} \\
& + \begin{bmatrix} I_c(\rho + \epsilon_\rho, \rho_2; 0, 2\pi; z - \epsilon_z, z + \epsilon_z) \\ I_\rho(\rho + \epsilon_\rho, \rho_2; 0, 2\pi; z - \epsilon_z, z + \epsilon_z) \\ I_z(\rho + \epsilon_\rho, \rho_2; 0, 2\pi; z - \epsilon_z, z + \epsilon_z) \end{bmatrix} \\
& + \begin{bmatrix} I_c(\rho - \epsilon_\rho, \rho + \epsilon_\rho; \epsilon_\phi, 2\pi - \epsilon_\phi; z - \epsilon_z, z + \epsilon_z) \\ I_\rho(\rho - \epsilon_\rho, \rho + \epsilon_\rho; \epsilon_\phi, 2\pi - \epsilon_\phi; z - \epsilon_z, z + \epsilon_z) \\ I_z(\rho - \epsilon_\rho, \rho + \epsilon_\rho; \epsilon_\phi, 2\pi - \epsilon_\phi; z - \epsilon_z, z + \epsilon_z) \end{bmatrix} \\
& + \begin{bmatrix} I_c^{sing} \\ I_\rho^{sing} \\ I_z^{sing} \end{bmatrix} \tag{73}
\end{aligned}$$

where I_c^{sing} , I_ρ^{sing} , and I_z^{sing} are integrals of the singular kernels in the small volume. The first five terms on the right-hand side involve no singularities and can be calculated numerically. The limits of the integrals in Eq. (73) can be better visualized with the aid of Fig. 7. The volume of the singular region is calculated as

$$V_{sing} = \int_{z-\epsilon_z}^{z+\epsilon_z} dz' \int_{\rho-\epsilon_\rho}^{\rho+\epsilon_\rho} d\rho' \rho' \int_{-\epsilon_\phi}^{\epsilon_\phi} d\phi' = 8\rho\epsilon_\rho\epsilon_\phi\epsilon_z \tag{74}$$

The singular region can be approximated by a small sphere centered at the singularity with a radius of

$$r_{sing} = \left(\frac{6}{\pi} \rho \epsilon_\rho \epsilon_\phi \epsilon_z \right)^{\frac{1}{3}} \tag{75}$$

which provides an equal volume. Assuming $\epsilon = \epsilon_\rho = \rho\epsilon_\phi = \epsilon_z$, the integral functions I_c^{sing} , I_ρ^{sing} , and I_z^{sing} can be calculated as

$$I_c^{sing} = \int_0^{r_{sing}} r'^2 dr' \int_0^\pi d\theta \sin \theta \int_0^{2\pi} d\phi' \frac{1}{r'} = 2(6\sqrt{\pi})^{\frac{2}{3}} \epsilon^2 \tag{76}$$

$$I_\rho^{sing} = \int_0^{r_{sing}} r'^2 dr' \int_0^\pi d\theta \sin \theta \int_0^{2\pi} d\phi' \frac{\rho + r' \sin \theta}{r'} = 2\epsilon^2 \left(\rho (6\sqrt{\pi})^{\frac{2}{3}} + \pi \epsilon \right) \tag{77}$$

$$I_z^{sing} = \int_0^{r_{sing}} r'^2 dr' \int_0^\pi d\theta \sin \theta \int_0^{2\pi} d\phi' \frac{r' \cos \theta}{r'} = 2\pi \epsilon^3 \tag{78}$$

II. GREEN'S FUNCTION WHEN THE SOURCE AND OBSERVATION POINTS ARE ON THE SOIL SURFACE

When the source and observation points are on the soil surface, i.e., $z = 0$ and $z' = 0$, the Green's function given by Eq. (43) can be simplified as

$$G(\rho, z = 0; \rho', z' = 0) = \int_0^\infty dk_\rho J_0(k_\rho \rho') J_0(k_\rho \rho) \frac{k_\rho}{\sqrt{k_n^2 + k_\rho^2} + \alpha} \quad (79)$$

Without the exponential factors, this integral converges slowly. The following approximation is valid for small α

$$\begin{aligned} \frac{1}{\sqrt{k_n^2 + k_\rho^2} + \alpha} &= \frac{1}{\sqrt{k_n^2 + k_\rho^2}} \frac{1}{1 + \frac{\alpha}{\sqrt{k_n^2 + k_\rho^2}}} \\ &\approx \frac{1}{\sqrt{k_n^2 + k_\rho^2}} \left(1 - \frac{\alpha}{\sqrt{k_n^2 + k_\rho^2}} + \frac{\alpha^2}{k_n^2 + k_\rho^2} - \frac{\alpha^3}{(k_n^2 + k_\rho^2)^{\frac{3}{2}}} \right) \end{aligned} \quad (80)$$

Substituting Eq. (80) into Eq. (79), employing the multiplication identity for the zeroth order Bessel functions given by Eq. (49), and changing the orders of ϕ and k_ρ integrals we obtain

$$\begin{aligned} G(\rho, z = 0; \rho', z' = 0) &\approx \frac{1}{2\pi} \int_0^{2\pi} d\phi' \int_0^\infty dk_\rho J_0(k_\rho \rho_t) \frac{k_\rho}{\sqrt{k_n^2 + k_\rho^2}} \\ &\quad - \alpha \int_0^\infty dk_\rho J_0(k_\rho \rho') J_0(k_\rho \rho) \frac{k_\rho}{k_n^2 + k_\rho^2} \\ &\quad + \frac{\alpha^2}{2\pi} \int_0^{2\pi} d\phi' \int_0^\infty dk_\rho J_0(k_\rho \rho_t) \frac{k_\rho}{(k_n^2 + k_\rho^2)^{\frac{3}{2}}} \\ &\quad - \frac{\alpha^3}{2\pi} \int_0^{2\pi} d\phi' \int_0^\infty dk_\rho J_0(k_\rho \rho_t) \frac{k_\rho}{(k_n^2 + k_\rho^2)^2} \end{aligned} \quad (81)$$

The k_ρ integrals in Eq. (81) can be evaluated in closed form [30–32], leading to

$$\begin{aligned} G(\rho, z = 0; \rho', z' = 0) &\approx \frac{1}{2\pi} \int_0^{2\pi} d\phi' \frac{\exp(ik_n \rho_t)}{\rho_t} - \alpha K_0(-ik_n \rho_{>}) I_0(-ik_n \rho_{<}) \\ &\quad - \frac{\alpha^2}{2\pi} \int_0^{2\pi} d\phi' \frac{\exp(ik_n \rho_t)}{ik_n} - \frac{\alpha^3}{4\pi} \int_0^{2\pi} d\phi' \frac{\rho_t K_{-1}(-ik_n \rho_t)}{ik_n} \end{aligned} \quad (82)$$

where K_0 , K_{-1} , and I_0 are modified Bessel functions.

ACKNOWLEDGMENTS

This project was supported by funds from Duke University under an award from the ARO (the OSD MURI program). The findings, opinions and recommendations expressed herein are those of the author and are not necessarily those of Duke University or the ARO.

REFERENCES

- [1] K. Watson, "Geologic application of thermal infrared images," *Proc. IEEE*, vol. 63, no. 1, pp. 128–137, Jan. 1975.
- [2] H. S. Carslaw and J. C. Jaeger, *Conduction of Heat in Soils*, Oxford Univ. Press, New York, NY, 1953.
- [3] A. W. England, J. F. Galantowicz, and M. S. Schretter, "The radiobrightness thermal inertia measure of soil moisture," *IEEE Trans. Geosci. Remote Sensing*, vol. 30, no. 1, pp. 132–139, Jan. 1992.
- [4] A. B. Kahle, "A simple thermal model of the earth's surface for geologic mapping by remote sensing," *Journal of Geophysical Research*, vol. 82, pp. 1673–1680, 1977.
- [5] K. Watson, "Periodic heating of a layer over a semi-infinite solid," *Journal of Geophysical Research*, vol. 78, no. 26, pp. 5904–5910, Sept. 1973.
- [6] Y.-A. Liou and A. W. England, "Annual temperature and radiobrightness signatures for bare soils," *IEEE Trans. Geosci. Remote Sensing*, vol. 34, no. 4, pp. 981–990, July 1996.
- [7] A. W. England, "Radiobrightness of diurnally heated, freezing soil," *IEEE Trans. Geosci. Remote Sensing*, vol. 28, no. 4, pp. 464–476, July 1990.
- [8] Y.-A. Liou and A. W. England, "A land-surface process/radiobrightness model with coupled heat and moisture transport in soil," *IEEE Trans. Geosci. Remote Sensing*, vol. 36, no. 1, pp. 273–286, Jan. 1998.
- [9] Y.-A. Liou and A. W. England, "A land-surface process/radiobrightness model with coupled heat and moisture transport for freezing soils," *IEEE Trans. Geosci. Remote Sensing*, vol. 36, no. 2, pp. 669–677, March 1998.
- [10] I. K. Sendur and B. A. Baertlein, "Thermal analysis of IR signatures for buried land mines," Progress Report to US Army Research Office on Contract 97-SC-ARO-1015, The Ohio State University ElectroScience Laboratory, Columbus, OH, March 1999.
- [11] I. K. Sendur and B. A. Baertlein, "Three-dimensional thermal modeling of land mine signatures over a diurnal cycle," *submitted to IEEE Trans. Geo. Rem. Sens.*
- [12] I. Stakgold, *Green's Functions and Boundary Value Problems*, Academic Press, 1980.
- [13] C. A. Balanis, *Advanced Engineering Electromagnetics*, John Wiley and Sons, 1989.
- [14] W. C. Chew, *Waves and Fields in Inhomogeneous Media*, IEEE Press, 1995.
- [15] J. A. Kong, *Electromagnetic Wave Theory*, John Wiley and Sons, 1986.
- [16] A. Sommerfeld, *Partial Differential Equation in Physics*, Academic Press, 1949.
- [17] W. A. Johnson, "Analysis of a vertical, tubular cylinder which penetrates an air-dielectric interface and which is excited by an azimuthally symmetric source," *Radio Science*, vol. 18, no. 6, pp. p. 1273–1281, 1983.
- [18] W. C. Kuo and K. K. Mei, "Numerical approximations of the Sommerfeld integral for fast convergence," *Radio Science*, vol. 13, no. 3, pp. p. 407–415, 1978.
- [19] J. H. Richmond, "Digital computer solutions of the rigorous equations for scattering problems," *Proc. IEEE*, vol. 53, pp. p. 796–804, 1965.

- [20] R. F. Harrington, "Matrix methods for field problems," *Proc. IEEE*, vol. 55, no. 2, pp. p. 136–149, 1967.
- [21] R. F. Harrington, *Field Computation by Moment Methods*, IEEE Press, 1993.
- [22] E. K. Miller, L. Medgyesi-Mitschang, and E. H. Newman, Eds., *Computational Electromagnetics*, IEEE Press, 1992.
- [23] R. C. Hansen, Ed., *Moment Methods in Antennas and Scattering*, Artech, 1990.
- [24] D. R. Wilton, S. M. Rao, A. W. Glisson, D. H. Schaubert, O. M. Al-Bundak and C. M. Butler, "Potential integrals for uniform and linear source distributions on polygonal and polyhedral domains," *IEEE Trans. Antennas Propagat.*, vol. 32, no. 2, pp. p. 276–281, 1984.
- [25] D. E. Livesay, and K. M. Chen, "Electromagnetic fields induced inside arbitrarily shaped biological bodies," *IEEE Trans. Microwave Theory Tech.*, vol. 22, no. 12, pp. p. 1273–1280, 1974.
- [26] S. M. Rao, D. R. Wilton, and A. W. Glisson, "Electromagnetic scattering by surfaces of arbitrary shape," *IEEE Trans. Antennas Propagat.*, vol. 30, pp. p. 409–418, 1982.
- [27] D. H. Schaubert, D. R. Wilton, and A. W. Glisson, "A tetrahedral modeling method for electromagnetic scattering by arbitrarily shaped inhomogeneous dielectric bodies," *IEEE Trans. Antennas Propagat.*, vol. 32, no. 1, pp. p. 77–85, 1984.
- [28] T. K. Sarkar, "A study of the various methods for computing electromagnetic field utilizing thin wire integral equations," *Radio Science*, vol. 18, pp. p. 29–38, 1983.
- [29] M. G. Andreasen, "Scattering from bodies of revolution," *IEEE Trans. Antennas Propagat.*, vol. 13, no. 2, pp. p. 303–310, 1965.
- [30] I. S. Gradshteyn and I. M. Ryzhik, *Table of Integrals, Series, and Products*, Academic Press, 1980.
- [31] A. Erdelyi, *Tables of Integral Transforms*, vol. 2, Mc-Graw Hill, 1954.
- [32] G. N. Watson, *A Treatise on the Theory of Bessel Functions*, Cambridge University Press, 1945.

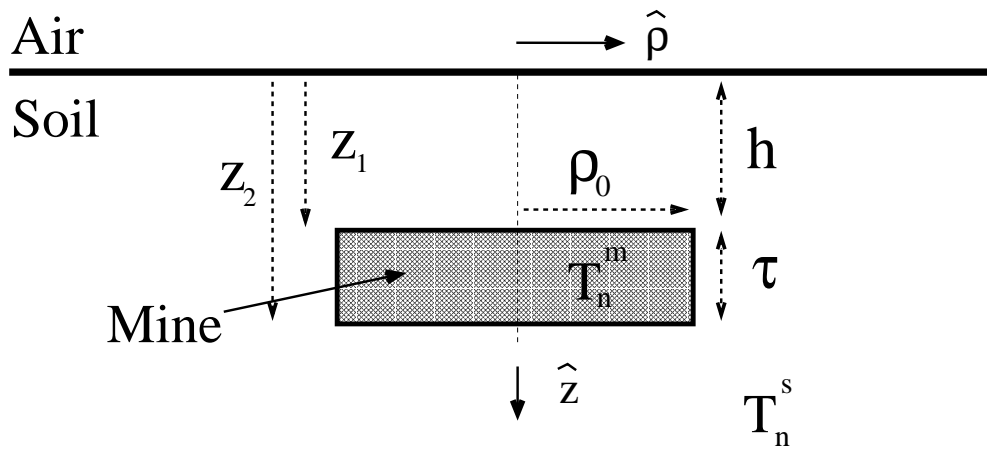


Fig. 1. A cylindrical mine with radius ρ_0 and thickness τ , buried at depth h under a smooth soil surface. The Fourier series coefficients in the mine and soil regions are represented with $T_n^m(\mathbf{r})$ and $T_n^s(\mathbf{r})$, respectively.

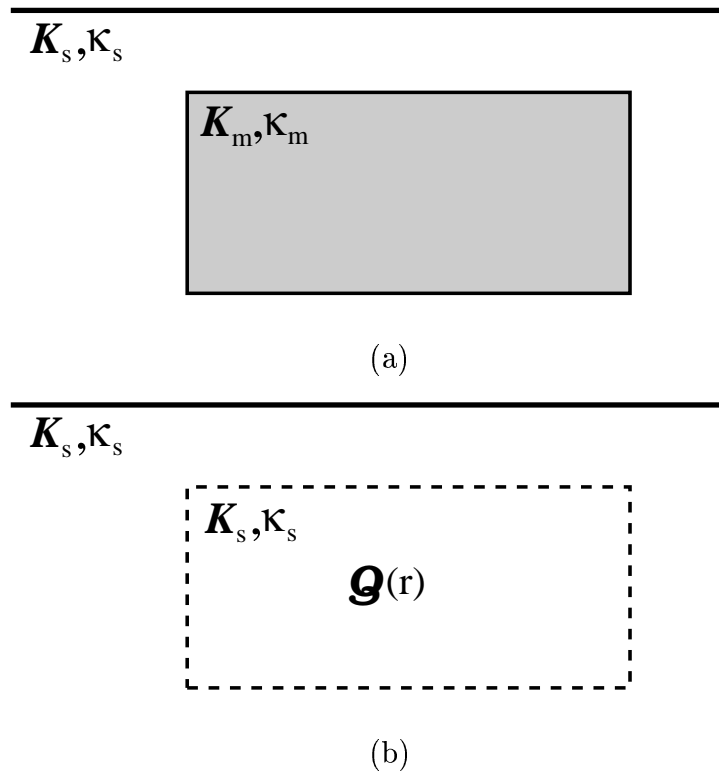


Fig. 2. Volume equivalence for heat transfer equation. (a) The original problem, in which a buried mine with thermal properties $\kappa_m(\mathbf{r})$ and $\mathcal{K}_m(\mathbf{r})$ is present in homogeneous soil with thermal properties $\kappa_s(\mathbf{r}) = \kappa_s$ and $\mathcal{K}_s(\mathbf{r}) = \mathcal{K}_s$. (b) The equivalent problem, in which the mine is replaced by homogeneous soil and an equivalent distributed heat source $\mathcal{Q}(\mathbf{r})$.

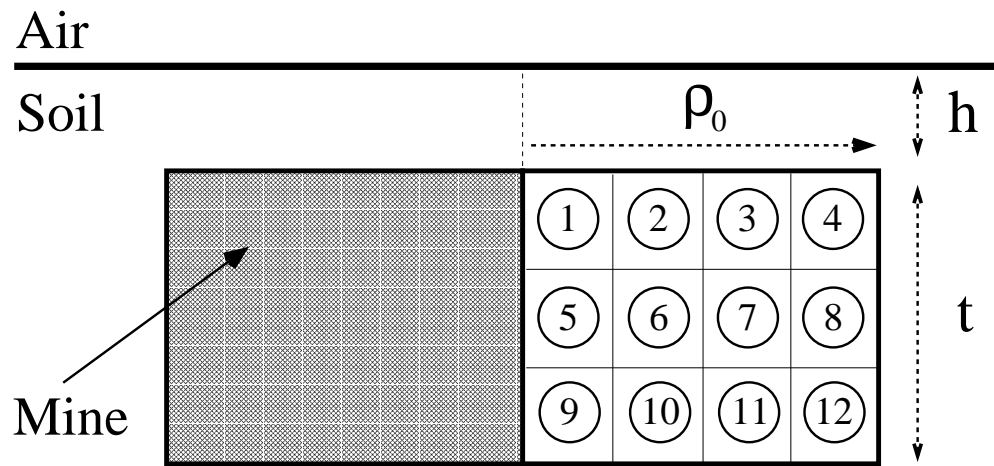


Fig. 3. An example discretization of the buried mine with 4 subdivisions in the $\hat{\rho}$ -direction and 3 subdivisions in the \hat{z} -direction

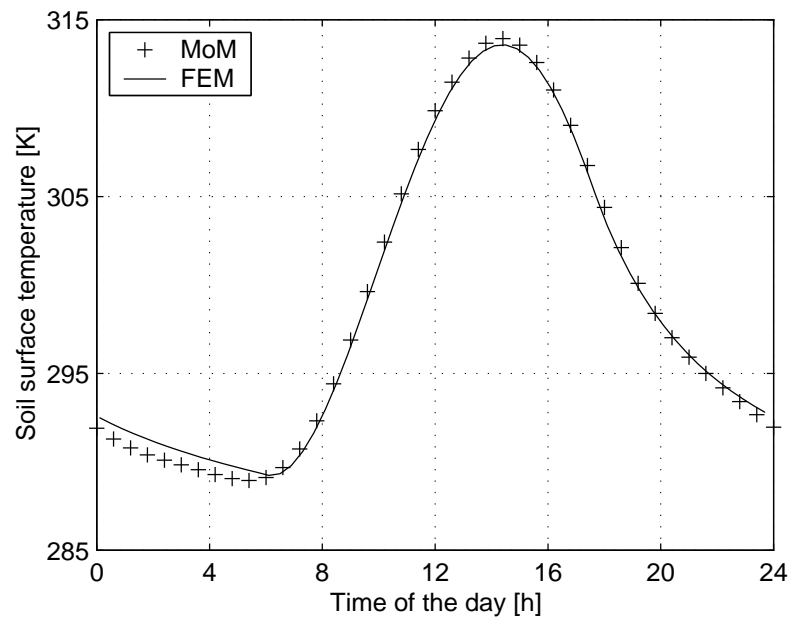
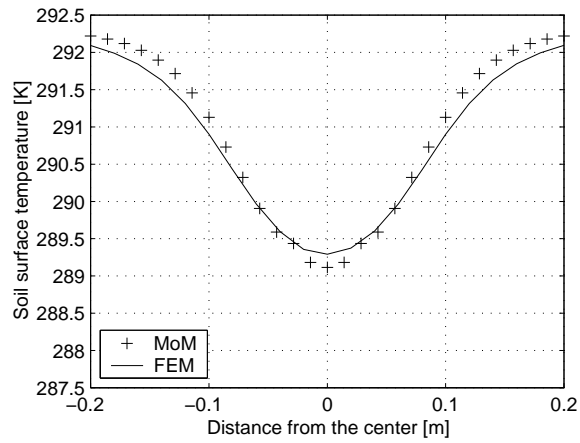
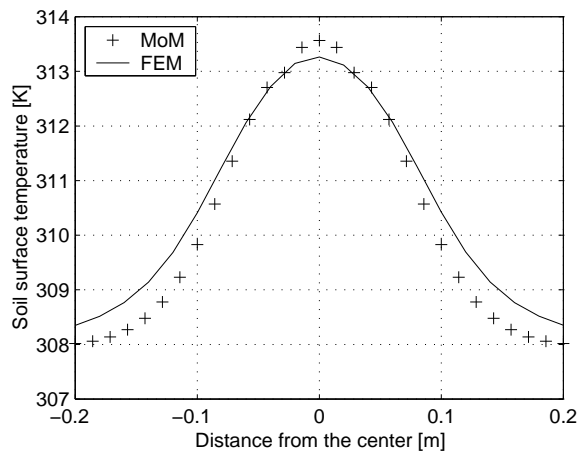


Fig. 4. The surface temperature distribution over the center of a cylindrical mine using the integral equation solution and a finite element solution.



(a)



(c)

Fig. 5. The spatial dependence of the surface temperature distribution: (a) When the mine signature has a maximum negative contrast, (b) When the mine signature has a maximum positive contrast.

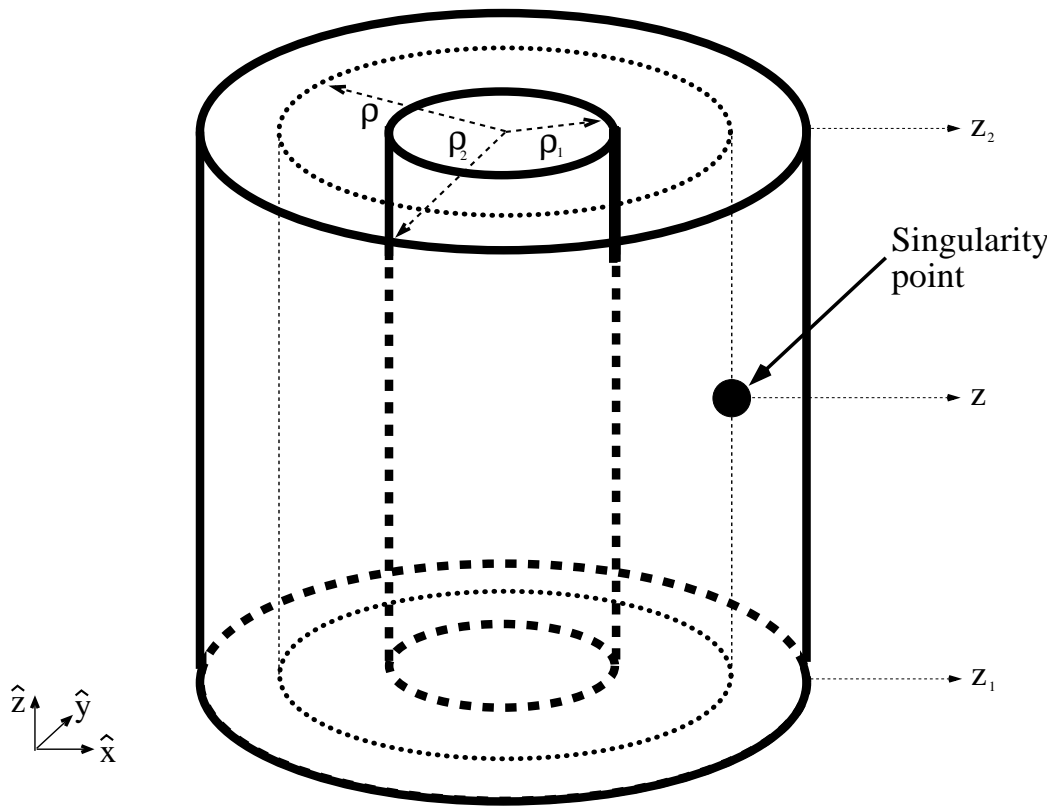
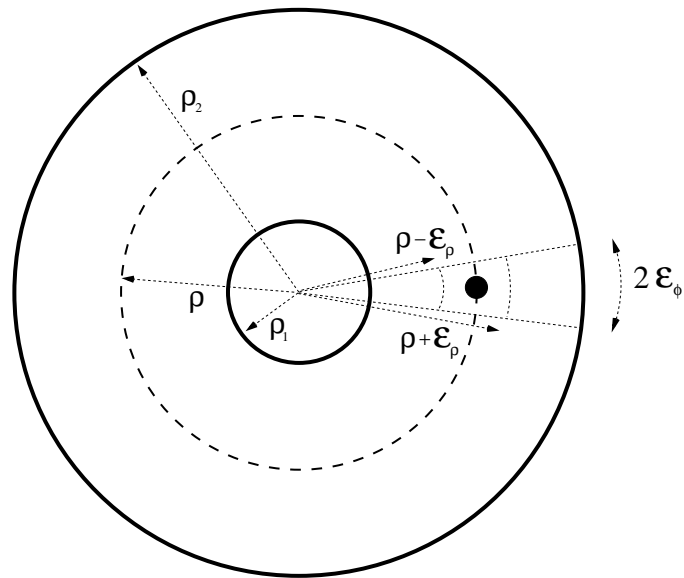
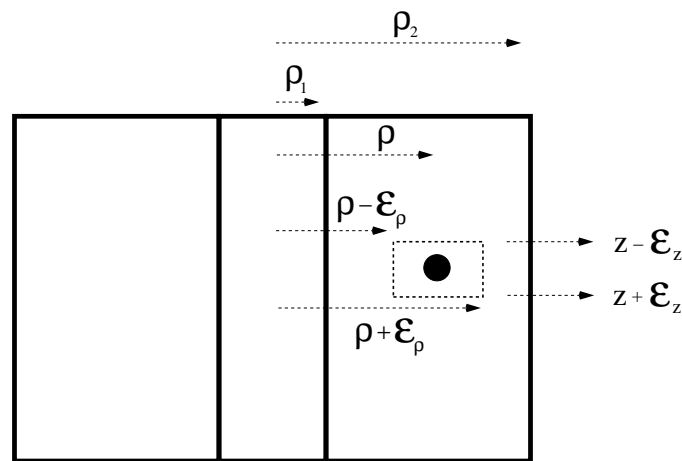


Fig. 6. The singularity point and the boundaries of the singular integral.



(a)



(b)

Fig. 7. The small volume around the singularity (a) Top view. (b) Side view.